Mem. S.A.It. Vol. 75, 706

Memorie della

Lead and s-process elements in stars of various metallicities: AGB predictions compared with observation

D. Delaude[1], R. Gallino[1], S. Cristallo[2], O. Straniero[2], L. Husti[3] and S. Ryan[4]

[1] Dipartimento di Fisica dell'Universitá di Torino, via P.Giuria 1, 10125 Torino, Italy
[2] Osservatorio Astronomico di Collurania, 64100 Teramo, Italy
[3] University of Bucharest, Romania
[4] Open University, Walton Hall, Milton Keynes, UK

Abstract. We present AGB predictions for all heavy elements within a large range of ^{13}C-pocket efficiencies for stars of different metallicities, and compare them in detail with a number of spectroscopic observations of *s*-rich and lead-rich in the Galaxy. The current concept of the *s*-process efficiency, specified by the [hs/ls] index, is shown to be inappropriate for the metal poor AGB stars and a second independent index, [Pb/hs] or [Pb/ls], needs to be introduced. The state-of-the-art concerning the interpretation of lead stars allows a very large spread of [Pb/hs] in metal poor stars, as typically observed. We discuss agreements and discrepancies for a large range of elements.

Key words. AGB stars – AGB nucleosynthesis – Lead stars – *s*-process

1. Introduction

Spectroscopic detection of lead requires very high-resolution spectroscopy. This is why lead-rich stars have only been observed in the last few years. As discussed in Travaglio et al. (2001), the *s*-process can bring forth a large production of lead in AGB stars at low metallicity. In fact lead and bismuth are at the termination points of the *s*-fluence. Using a primary-like neutron source (like the ^{13}C(α,n)^{16}O reaction in interpulse phases) and starting with a very low initial metallicity, most iron seeds are converted into ^{208}Pb. So, when third dredge up episodes mix the neutron capture products into the envelope, the star appears *s*-enhanced and lead-rich.

Send offprint requests to: R. Gallino
Correspondence to: gallino@ph.unito.it

2. The intrinsic index [Pb/hs]

Commonly s-rich stars are classified as either intrinsic or extrinsic, with extrinsic being those stars that become *s*-enhanced not because of internal nucleosynthesis but through receiving *s*-rich material from a companion in a binary system by mass transfer. To characterize neutron capture process efficiencies, without distinguishing between these two types of objects, usually the intrinsic index [hs/ls] is used (where hs is the average abundance of the heavy *s*-elements Ba, La, Nd, Sm, and ls of the light *s*-elements Y, Zr). However, at low metal-

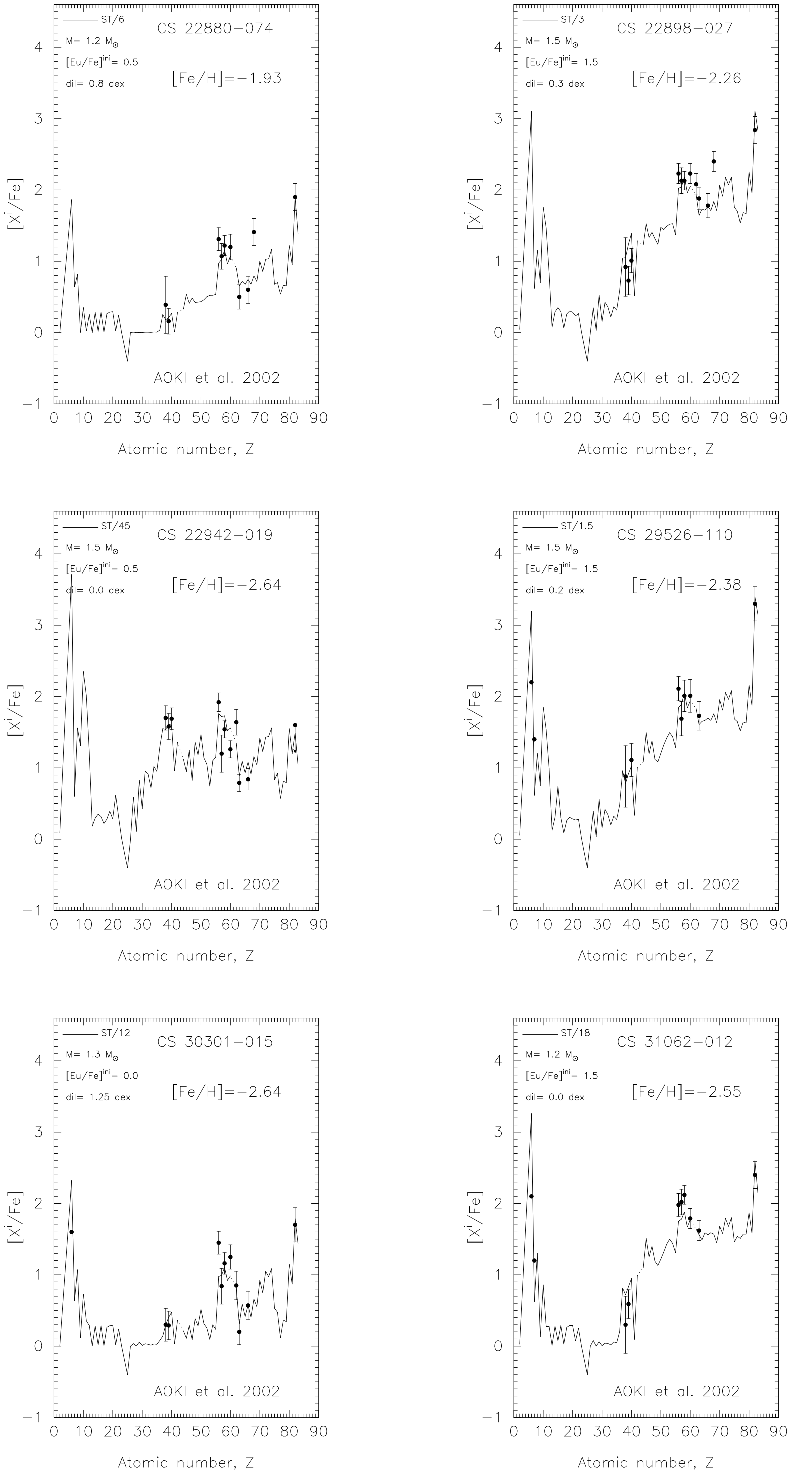
ST/6
M= 1.2 M⊙
[Eu/Fe]ini= 0.5
dil= 0.8 dex
CS 22880−074
[Fe/H]=−1.93
AOKI et al. 2002
[Xi/Fe]
Atomic number, Z
ST/3
M= 1.5 M⊙
[Eu/Fe]ini= 1.5
dil= 0.3 dex
CS 22898−027
[Fe/H]=−2.26
AOKI et al. 2002
[Xi/Fe]
Atomic number, Z
ST/45
M= 1.5 M⊙
[Eu/Fe]ini= 0.5
dil= 0.0 dex
CS 22942−019
[Fe/H]=−2.64
AOKI et al. 2002
[Xi/Fe]
Atomic number, Z
ST/1.5
M= 1.5 M⊙
[Eu/Fe]ini= 1.5
dil= 0.2 dex
CS 29526−110
[Fe/H]=−2.38
AOKI et al. 2002
[Xi/Fe]
Atomic number, Z
ST/12
M= 1.3 M⊙
[Eu/Fe]ini= 0.0
dil= 1.25 dex
CS 30301−015
[Fe/H]=−2.64
AOKI et al. 2002
[Xi/Fe]
Atomic number, Z
ST/18
M= 1.2 M⊙
[Eu/Fe]ini= 1.5
dil= 0.0 dex
CS 31062−012
[Fe/H]=−2.55
AOKI et al. 2002
[Xi/Fe]
Atomic number, Z

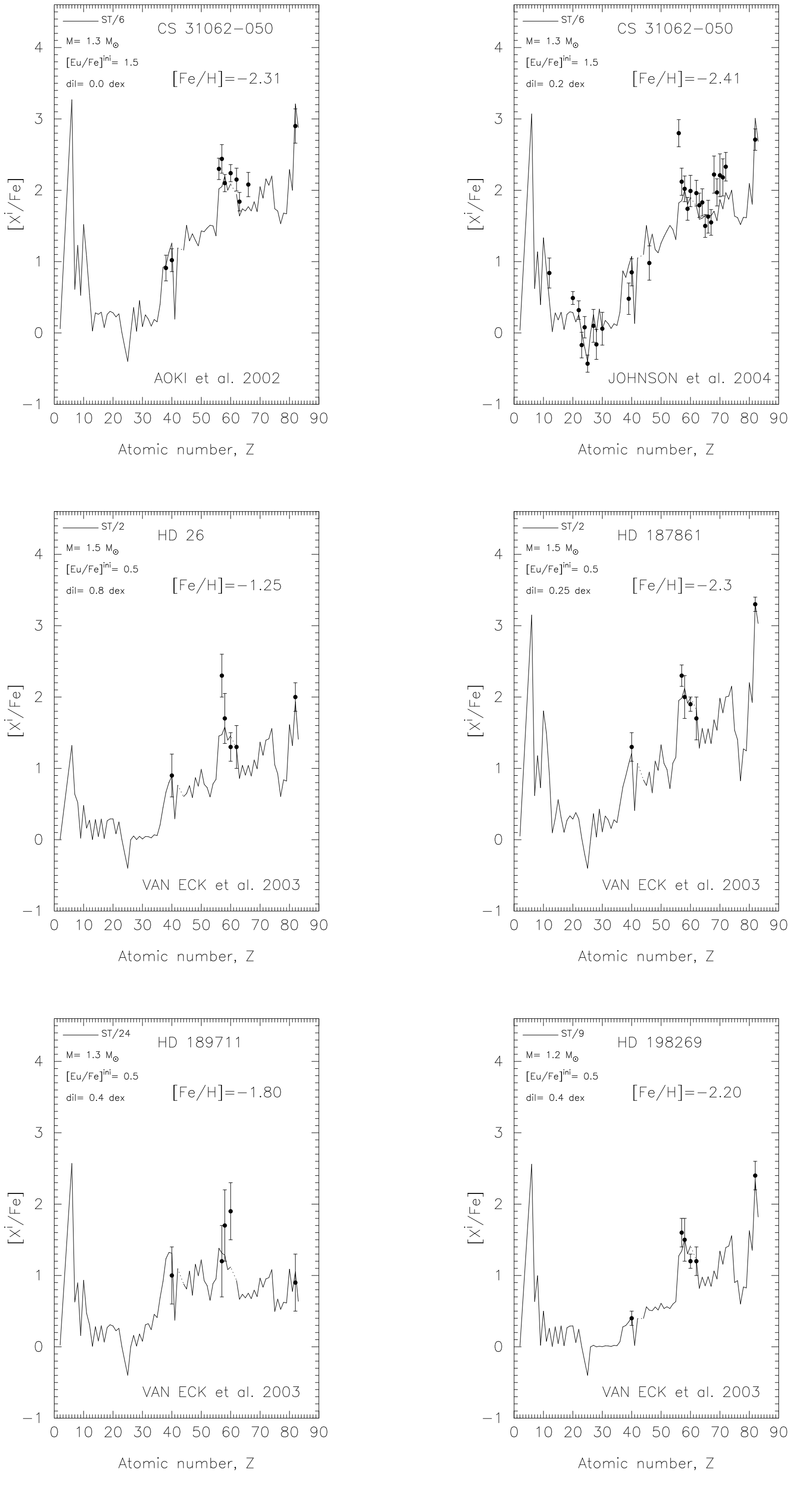
ST/6
M= 1.3 M⊙
[Eu/Fe]ini= 1.5
dil= 0.0 dex
CS 31062−050
[Fe/H]=−2.31
AOKI et al. 2002
ST/6
M= 1.3 M⊙
[Eu/Fe]ini= 1.5
dil= 0.2 dex
CS 31062−050
[Fe/H]=−2.41
JOHNSON et al. 2004
ST/2
M= 1.5 M⊙
[Eu/Fe]ini= 0.5
dil= 0.8 dex
HD 26
[Fe/H]=−1.25
VAN ECK et al. 2003
ST/2
M= 1.5 M⊙
[Eu/Fe]ini= 0.5
dil= 0.25 dex
HD 187861
[Fe/H]=−2.3
VAN ECK et al. 2003
ST/24
M= 1.3 M⊙
[Eu/Fe]ini= 0.5
dil= 0.4 dex
HD 189711
[Fe/H]=−1.80
VAN ECK et al. 2003
ST/9
M= 1.2 M⊙
[Eu/Fe]ini= 0.5
dil= 0.4 dex
HD 198269
[Fe/H]=−2.20
VAN ECK et al. 2003
[Xi/Fe]
Atomic number, Z

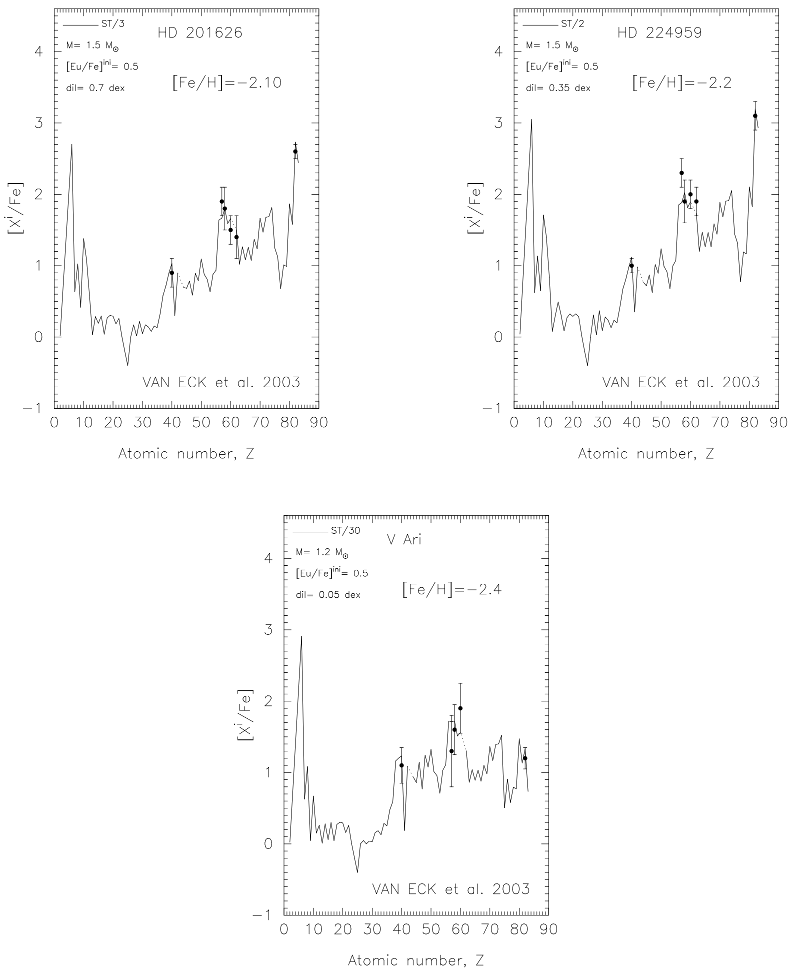

Fig. 4. Fits of a large sample of *s*-rich and lead-rich stars with AGB model predictions.

licities, another intrinsic index is required. In fact at decreasing metallicities [hs/Fe] and [ls/Fe] converge within a small range, while [Pb/Fe] always increases (see the figures in Gallino et al. 2004 - hereafter Paper I). Here, in Figure 1, [hs/ls] is plotted as a function of metallicity for various choices of ^{13}C-pockets. The standard case (ST) is the one that for [Fe/H]=−0.3 best reproduces the main component of the solar system (Gallino et al. 1998). Different ^{13}C-pockets can provide very similar [hs/ls] indices, but still show a large range of [Pb/ls] and [Pb/hs] values. These are plotted respectively in Figure 2 and Figure 3; for instance consider the cases ST*1.3 and ST/3 at [Fe/H]=−2.

3. Comparison of models with observations

Using AGB nucleosynthesis models with different ^{13}C-pockets efficiencies, initial masses and metallicities, we tried to fit the spectroscopic abundances of the *s*-rich and lead-rich stars listed in the Table of Paper I. The fit is made by comparing the element distribution observed in each star with the distribu-

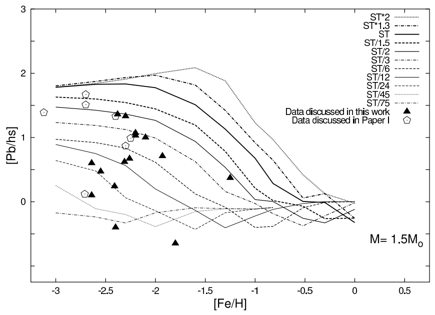

Fig. 3. [Pb/hs] versus [Fe/H] for different ^{13}C-pocket choices. Spectroscopic data of s-rich and lead-rich stars are included for comparison.

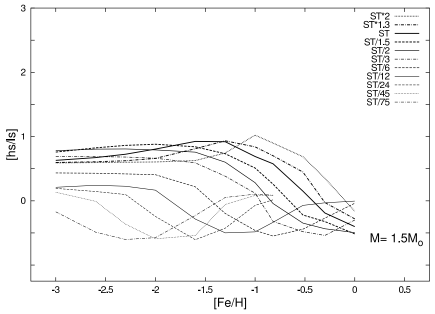

Fig. 1. [hs/ls] versus [Fe/H] for different ^{13}C-pocket choices.

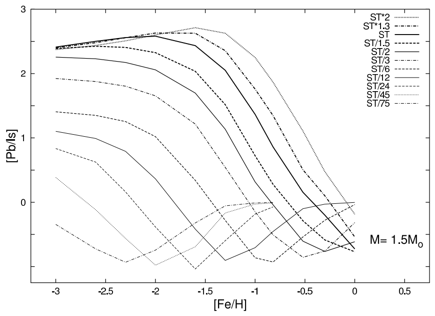

Fig. 2. [Pb/ls] versus [Fe/H] for different ^{13}C-pocket choices.

tion predicted by AGB models with different ^{13}C-pocket efficiencies. Such a large spread is justified by observation of MS, S, C(N), Ba stars in the disk (see Busso et. al 2001; Abia et al. 2002). In Figure 4 we report the fits of lead stars not yet presented in Paper I. To compare our predicted abundances with observations, in many cases we apply a dilution that simulates the effect of mixing of s-rich material in the envelope of extrinsic stars, using the rule: dil=log($M_{\rm env}^{\rm ini}/M_{\rm transf}$), where $M_{\rm env}^{\rm ini}$ is the initial envelope mass and $M_{\rm transf}$ is the mass of transfered material. The choice of ^{13}C-pocket efficiency, the initial mass, the initial [Eu/Fe] assumed (see below), the dilution factor and the metallicity are indicated in each plot. In AGB stars of low metallicity, the *s*-process feeds Eu at a consistent level, with a constant ratio $[\mathrm{Ba/Eu}]_s \sim 0.7$. For several lead stars the spectroscopic observation indicates a lower [Ba/Eu] ratio than predicted, which may imply a different $[\mathrm{Eu/Fe}]^{\rm ini}$ in the parent cloud. Indeed, unevolved halo stars in the same range of metallicity show an average [Eu/Fe] = 0.5, with a large spread Δ[Eu/Fe] = ± 0.5 dex (see Travaglio et al. 2004). The adopted $[\mathrm{Eu/Fe}]^{\rm ini}$ is indicated in each panel of Figure 4. Notice that the rule adopted for $[\mathrm{Eu/Fe}]^{\rm ini}$ has been applied also to other elements of major r-process origin, e.g. for all the elements from Eu to Tm. For the star CS 31062-050 (Johnson et al. 2004) lines of Cr and Mn have been detected, and somewhat negative [Cr/Fe] and [Mn/Fe] values have been deduced. The *s*-process in AGB stars produces very little Cr and Mn, however unevolved halo stars in the same range of metallicity show a depletion of both Cr and Mn, with an average [Cr/Fe]= −0.2 and [Mn/Fe]= −0.4 (see e.g., François et al. 2004). As shown in Figure 4 for CS 31062-050, adopting these initial values a satisfatory agreement is reached. For some stars, the observed [Ba/Fe] appears significantly higher than [La/Fe], whereas AGB models predict [Ba/Fe] $\simeq$ [La/Fe]. This may indicate difficulties in the determination of the Ba abundance. In general, lanthanum is a more representative element of the second *s*-peak at neutron magic number, $N = 82$.

In several cases we need to attain high [hs/ls] values without changing [Pb/hs]; according to our AGB models, those values can be reproduced using lower initial masses with respect to the standard mass of $1.5 M_{\odot}$. Reducing the initial mass corresponds to a decrease in the number of thermal pulses. From the previous discussion it is clear that a general comparison of AGB predictions with all the elements detected provides a better method rather than being restricted to the average ls or hs values. Anyway, in Figure 5 the hs data are compared with AGB predictions in the [Pb/hs] versus [Fe/H], showing that the large spread of spectroscopic data are well fitted within the large spread of ^{13}C-pocket efficiencies adopted.

4. Conclusion

A comparison is made of AGB model predictions of low metallicity with spectroscopic data of a large sample of s-rich and lead-rich stars. Varying the initial mass and adopting a large spread of ^{13}C-pocket efficiencies for a given metallicity a satisfactory reproduction of all data is obtained.

Acknowledgements. Part of this work was supported by the Italian MIUR-FIRB Project “Astrophysical Origin of the Heavy Elements beyond Fe”.

References

Abia C., et al., 2002, ApJ, 579, 817
Aoki W., et al., 2001, ApJ, 561, 346
Aoki W., et al., 2002, ApJ, 580, 1149
Busso M., et al., 2001, ApJ, 557, 802
Cohen J. G., et al., 2003, ApJ, 588, 1082
François P., et al., 2004, A&A, 421, 613
Gallino R., et al., 1998, ApJ, 497, 388
Gallino R., et al., 2004, Nucl. Phys. A, (in press) (Paper I)
Johnson J. A., Bolte M., 2002, ApJ, 579, L87
Johnson J. A., Bolte M., 2004, ApJ, 605, 462
Lucatello S., et al., 2003, AJ, 125, 875
Sivarani T., et al., 2004, A&A, 413, 1073
Travaglio C., et al., 2001, ApJ, 549, 346
Travaglio C., et al., 2004, ApJ, 601, 864
Van Eck S., et al., 2003, A&A, 404, 291